

Validation of a Mathematical Model for Road Cycling Power

*James C. Martin, Douglas L. Milliken, John E. Cobb,
Kevin L. McFadden, and Andrew R. Coggan*

This investigation sought to determine if cycling power could be accurately modeled. A mathematical model of cycling power was derived, and values for each model parameter were determined. A bicycle-mounted power measurement system was validated by comparison with a laboratory ergometer. Power was measured during road cycling, and the measured values were compared with the values predicted by the model. The measured values for power were highly correlated ($R^2 = .97$) with, and were not different than, the modeled values. The standard error between the modeled and measured power (2.7 W) was very small. The model was also used to estimate the effects of changes in several model parameters on cycling velocity. Over the range of parameter values evaluated, velocity varied linearly ($R^2 > .99$). The results demonstrated that cycling power can be accurately predicted by a mathematical model.

Key Words: aerodynamic drag, rolling resistance, air velocity, gradient

Several models of cycling performance have been presented in previous investigations (Davies, 1980; Di Prampero, Cortili, Mognoni, & Saibene, 1979; Kyle, 1988; Olds et al., 1995; Olds, Norton, & Craig, 1993). In general, these models have been based on physiological, anthropometric, and environmental parameters. The investigators have used these models to predict time trial performance and to predict how changes in modeling parameters might affect performance (di Prampero et al., 1979; Kyle, 1988; Olds et al., 1993, 1995). To our knowledge, however, no investigation has addressed the most fundamental question regarding modeling: Can a mathematical model accurately predict power during road cycling?

During cycling, the rider remains relatively fixed on the bicycle and essentially assumes the role of an engine, producing power to propel the bicycle. The external factors that impede motion of the bicycle/rider system can be modeled based on fundamental engineering and physical principles. These factors include aerodynamic drag, rolling resistance, friction in the bearings and chain drive system, and changes in kinetic and poten-

James C. Martin is with the Motor Control Laboratory, Department of Kinesiology and Health Education, The University of Texas at Austin, Austin, TX 78712. Douglas L. Milliken is with Milliken Research Associates, Inc., 245 Brompton Road, Williamsville, NY 14221. John E. Cobb is with Bicycle Sports, 288 South Field St., Shreveport, LA 71105. Kevin L. McFadden is with General Motors Vehicle Aerodynamics Laboratory, 6363 E. 12 Mile Rd., Warren, MI 48090. Andrew R. Coggan is with the Metabolism Unit, Shriners Burns Institute, and Department of Anesthesiology, University of Texas Medical Branch, Galveston, TX 77550.

tial energy. Of these factors, aerodynamic drag is often the largest resistance encountered during cycling and is related to the air density, frontal area, shape, and air velocity. Rolling resistance is related to the combined weight of the bicycle and rider, tire pressure and construction, road gradient, and road surface texture (Ryschon, 1994). Finally, changes in potential energy are related to mass, gravity, and vertical velocity, while changes in kinetic energy are related to mass, inertia, and velocity.

Previous models have accounted for up to 79% of the variation in cycling time trial performance (Olds et al., 1995). However, validation of these models has remained correlative, because none of these investigations measured power during road cycling. Previously, devices for measuring and recording cycling power required computer interfaces (Coyle et al., 1991; Wheeler, Gregor, & Broker, 1992) or did not record or provide a valid measure of power (Hooker & Spangler, 1989). Recently, the SRM Training System (Schoberer, 1994) has become available commercially and is claimed to be accurate to within $\pm 1\%$. This system consists of a number of strain gauges mounted within a deformable disc positioned between the crank arm and the chain ring, and a small handlebar-mounted computer. It records and stores power, speed, and pedaling rate data at 1 s intervals. If, in fact, this device is capable of measuring power accurately and storing the data, it can be used to determine if mathematical modeling accurately predicts cycling power.

The purpose of this investigation was to determine if cycling power, measured during actual road cycling, can be accurately predicted by a mathematical model. Achieving that goal required four tasks: (a) Establish whether the SRM power measurement system provided a valid measure of cycling power, (b) derive a mathematical model of cycling power based on engineering and physical principles, (c) determine values for each parameter in the model, and (d) compare the power values predicted by the model with the directly measured values.

Methods

Methods employed in this investigation were designed to accomplish the four tasks stated above. The first step was to determine if the SRM power measurement system provided a valid measure of cycling power. This was accomplished by comparing the SRM power with a known "gold standard": a Monark cycle ergometer. Next we developed a mathematical model of cycling power based on engineering and physical principles, such that all of the relevant parameters could be measured directly or determined from previous investigations. Third, we determined each parameter required by the model for the 6 subjects in this investigation. Fourth, we measured the power of our 6 subjects during road cycling trials at several velocities. Last, we compared the cycling power recorded during road cycling trials with the power estimated by the mathematical model to determine the validity and accuracy of our model.

Validation of the SRM Power Measurement System

The SRM was mounted on a Monark cycle ergometer (Model 818). The ergometer was calibrated by hanging known weights on the belt and observing the deflection of the pendulum. The SRM was set to zero according to the manufacturer's recommended procedure (Schoberer, 1994). The "zero" was set with the chain removed from the drive system so that chain friction would be included in the measured power.

Following calibration, a subject pedaled the ergometer for 3 min stages at six different work rates (45, 90, 135, 180, 225, and 270 W) at 90 RPM. Twenty seconds was al-

lowed between each work rate for the pendulum to be adjusted, resulting in 160 s of data for each workload. The pendulum was continuously monitored and adjusted to maintain the proper load. The subject pedaling the ergometer was an experienced cyclist and was instructed to maintain a constant pedaling rate throughout the trial. SRM data for power and pedaling rate were recorded at 1 s intervals.

From the SRM data, the pedaling rate at each 1 s interval was used in conjunction with the load on the ergometer pendulum to calculate the power delivered to the flywheel as

$$P_{FW} = PR \times GR \times R_{FW} \times L / 9.55 = \omega \times R_{FW} \times L$$

where P_{FW} is power delivered to the flywheel, PR is pedaling rate, GR is the gear ratio of the ergometer, R_{FW} is the radius of the flywheel, L is load (newtons) represented by the displacement of the pendulum, 9.55 is a factor to convert RPM to rad/s, and ω is angular velocity of the flywheel calculated from pedaling rate and gear ratio ($\omega = PR \times GR/9.55$).

Additionally, power associated with changes in the kinetic energy stored in the flywheel was calculated by finite difference methods:

$$P_i = I_{FW} \times \omega_i \times (\omega_{i+1} - \omega_{i-1})/2,$$

where P_i is the power associated with flywheel acceleration at time i , I_{FW} is the moment of inertia of the flywheel ($0.95 \text{ kg} \cdot \text{m}^2$), and $i+1$ and $i-1$ represent conditions 1 s after and 1 s before the time i .

Thus, total power delivered to the ergometer flywheel (P_{FWT}) was calculated as the sum of these two equations:

$$P_{FWT} = \omega_i \times R_{FW} \times L + I_{FW} \times \omega_i \times (\omega_{i+1} - \omega_{i-1})/2$$

Derivation of a Mathematical Model

The power required to propel a bicycle and rider can be modeled using fundamental engineering and physical principles. Our model includes terms for the power required to overcome aerodynamic drag, rolling resistance, wheel bearing friction, the rate of change of potential and kinetic energy, and friction in the drive chain.

Aerodynamic Resistance. Aerodynamic drag force (F_D) is related to the frontal area and shape of the bike and rider and to the air density and air velocity (Fox & McDonald, 1973) as described by Equation 1:

$$F_D = 1/2 \rho C_D A V_a^2 \quad (1)$$

where ρ is air density, C_D is the coefficient of drag, A is the frontal area, and V_a is air velocity tangent to the direction of travel of the bike and rider (which is dependent on wind velocity and direction and the ground velocity of the bicycle).

Drag force, air velocity, and air density were measured in the Texas A&M wind tunnel (see Determination of Model Parameters, below). From those measured variables, the product of $C_D \times A$ (drag area) was then calculated ($C_D A = 2F_D/\rho V_a^2$) and used to estimate drag force as a function of air density and velocity. Power is the product of force and velocity; therefore, the power to overcome aerodynamic drag is the product of F_D and the ground velocity of the bike and rider (V_G), as shown in Equation 2.

$$P_{AD} = 1/2 \rho C_D A V_a^2 V_G \quad (2)$$

Drag area varies with the direction of the air stream relative to the bike and rider (i.e., cross-winds affect drag). Therefore, yaw angle must be calculated for each set of

conditions in the model. The wind velocity was divided into components that are tangent (V_{WTAN}) and normal (V_{WNOR}) to the direction of travel of the bicycle, as shown below.

$$V_{WTAN} = V_w [\text{COS}(D_w - D_b)], \text{ and}$$

$$V_{WNOR} = V_w [\text{SIN}(D_w - D_b)]$$

where V_w is the absolute wind velocity (m/s), D_w is the wind direction, and D_b is the direction of travel of the bicycle.

The air velocity of the bicycle was calculated by adding ground and wind velocity as shown below.

$$V_a = V_G + V_{WTAN}$$

The yaw angle of the bike and rider relative to the wind was calculated as

$$\text{Yaw angle} = \text{TAN}^{-1}(V_{WNOR}/V_a)$$

This calculated value of yaw angle was used to select the proper value of drag area (see Determination of Model Parameters, below) by linear interpolation between the measured values.

Wheel Rotation. An additional aerodynamic power term associated with rotating the wheels is not measured by the wind tunnel balance. Specifically, as the wheels rotate, the spokes slice through the air like the blades of a fan. We measured this component of aerodynamic power (P_w) by using the SRM crank to rotate wheels with the bicycle suspended above the ground. Data were recorded for the rear wheel used in the trials and for a rear version of the front wheel used. This technique allowed us to measure both aerodynamic power to rotate the wheel and frictional power lost to chain and bearing friction. Therefore, the power required to rotate a hub (P_H) with no wheel was also measured. This value was subtracted from the power to rotate the rear wheel to obtain the actual aerodynamic power required for wheel rotation ($P_{WR} = P_w - P_H$). Wheel rotation power was modeled as shown by Equation 3.

$$P_{WR} = 1/2 \rho F_w V_a^2 V_G \quad (3)$$

where F_w is a factor associated with wheel rotation that represents the incremental drag area of the spokes (m^2).

The total aerodynamic power (P_{AT}) associated with the bike and rider and with the rotating wheels is given by summing Equations 2 and 3 to form Equation 4.

$$P_{AT} = 1/2 \rho (C_D A + F_w) V_a^2 V_G \quad (4)$$

Rolling Resistance. The force due to rolling resistance (F_{RR}) is related to the weight of the bike and rider, tire pressure, tread pattern, casing construction, and gradient and texture of the riding surface. The effects of tire and surface characteristics are usually expressed as the coefficient of rolling resistance (C_{RR}), which is the ratio of the tangential force to the normal force. Thus, the force due to rolling resistance (F_{RR}) was calculated as shown in Equation 5, and it was assumed that C_{RR} did not vary with velocity.

$$F_{RR} = \text{COS}[\text{TAN}^{-1}(G_R)] C_{RR} m_T g \quad (5)$$

where m_T is total mass of bike and rider (kg), g is the acceleration of gravity (9.81 m/s²), and G_R is the road gradient (rise/run).

It follows that the power to overcome rolling resistance is given by Equation 6.

$$P_{RR} = V_G \text{COS}[\text{TAN}^{-1}(G_R)] C_{RR} m_T g \quad (6)$$

For typical road grades of up to 10%, $\text{COS}[\text{TAN}^{-1}(G_R)]$ is approximately 1 (0.995 to 1.0). Therefore, the simplified model shown in Equation 6a is justified for most road conditions.

$$P_{RR} = V_G C_{RR} m_T g \quad (6a)$$

Frictional Losses in Wheel Bearings. Dahn, Mai, Poland, and Jenkins (1991) measured the friction associated with bicycle wheel bearings and found that bearing friction was related to load and rotational speed. For wheel bearings, the torque in each bearing pair was $T = 0.015 + 0.00005N$, where N is rotational velocity in RPM, and torque is expressed in $N \cdot m$. Using this relation in conjunction with the tire diameter, we derived the following equation for the total power lost to bearing friction torque (P_{WB}) as a function of bicycle velocity.

$$P_{WB} = V_G (91 + 8.7V_G) 10^{-3} \quad (7)$$

Changes in Potential Energy. When riding up or down a hill, work is done against, or by, gravity. This work (W_{PE}) is related to the mass of the bike and rider, and the change in elevation, by Equation 8.

$$W_{PE} = D m_T g \text{ SIN} [\text{TAN}^{-1}(G_R)] \quad (8)$$

where D is the distance traversed.

Therefore, the power associated with changes in potential energy (P_{PE}) is related to mass and the vertical component of velocity as given by Equation 9.

$$P_{PE} = V_G m_T g \text{ SIN} [\text{TAN}^{-1}(G_R)] \quad (9)$$

For typical road grades of up to 10%, $\text{SIN}[\text{TAN}^{-1}(G_R)]$ is approximately G_R . Therefore, a simplified model is justified for most road conditions, as shown in Equation 9a.

$$P_{PE} = V_G G_R m_T g \quad (9a)$$

Changes in Kinetic Energy. Kinetic energy stored in a moving body is related to mass and velocity by the equation $\text{KE} = 1/2 m V^2$. When the velocity of the bike and rider changes, work must be done to, or by, the system according to Equation 10.

$$W_{KE} = \Delta \text{KE} = 1/2 m_T (V_{Gf}^2 - V_{Gi}^2) \quad (10)$$

where V_{Gi} is the initial ground velocity (m/s), and V_{Gf} is the final ground velocity.

Power related to changes in kinetic energy (P_{KE}) is the rate of change of kinetic energy as described by Equation 11.

$$P_{KE} = \Delta \text{KE} / \Delta t = 1/2 m_T (V_{Gf}^2 - V_{Gi}^2) / (t_f - t_i) \quad (11)$$

where t_i is the initial time and t_f is the final time.

There is additional kinetic energy stored in the rotating wheels ($\text{KE} = 1/2 I \omega^2$), where I is the moment of inertia of the two wheels (approximately $0.14 \text{ kg} \cdot \text{m}^2$) and ω is the angular velocity of the wheels. The angular velocity of the wheels is proportional to V_G as $\omega = V_G / r$, where r is the outside radius of the tire. Therefore, the kinetic energy stored in the wheels can be expressed as $\text{KE} = 1/2 I V_G^2 / r^2$. Adding this term to Equation 11 yields

$$P_{KE} = \Delta \text{KE} / \Delta t = 1/2 (m_T + I/r^2) (V_{Gf}^2 - V_{Gi}^2) / (t_f - t_i) \quad (12)$$

Summing Equations 4, 6, 7, 9, and 12 yields the following equation for net cycling power:

$$\begin{aligned}
 P_{NET} &= P_{AT} + P_{RR} + P_{WB} + P_{PE} + P_{KE} = \\
 P_{NET} &= V_a^2 V_G / 2 \rho (C_D A + F_w) + V_G C_{RR} m_T g \text{COS}[\text{TAN}^{-1}(G_R)] + \\
 &V_G (91 + 8.7 V_G) 10^{-3} + V_G m_T g \text{SIN}[\text{TAN}^{-1}(G_R)] + \\
 &1/2 (m_T + I/r^2) (V_{GT}^2 - V_{GI}^2) / (t_1 - t_r) \quad (13)
 \end{aligned}$$

Frictional Loss in the Drive Chain. Frictional losses occur in the drive chain and are related to the power transmitted. Since this loss occurs between the crank and the rear wheel, it can be viewed as a chain efficiency factor (E_c). No attempt was made to model friction in the crank axle bearings, because it was not possible (with our methods) to distinguish between bearing friction and chain losses. Therefore, the net estimated power must be divided by the chain efficiency as described in Equation 14 below. Consequently, the power lost to chain friction is the product of chain efficiency and net power ($P_c = P_{NET} \times E_c$). We assumed that efficiency was constant across the range of power measured.

$$P_{TOT} = [V_a^2 V_G / 2 \rho (C_D A + F_w) + V_G C_{RR} m_T g \text{COS}(\text{TAN}^{-1}(G_R)) + V_G (91 + 8.7 V_G) 10^{-3} + V_G m_T g \text{SIN}(\text{TAN}^{-1}(G_R)) + 1/2 (m_T + I/r^2) (v_t^2 - v_i^2) / (t_1 - t_r)] / E_c \quad (14)$$

If the reduced expressions (6a and 9a) are substituted, the equation becomes

$$P_{TOT} = [V_a^2 V_G / 2 \rho (C_D A + F_w) + V_G C_{RR} m_T g + V_G (91 + 8.7 V_G) 10^{-3} + V_G m_T g G_R + 1/2 (m_T + I/r^2) (V_{GT}^2 - V_{GI}^2) / (t_1 - t_r)] / E_c \quad (15)$$

If all of the model parameters can be accurately determined, these equations should provide an accurate prediction of power during road cycling. A detailed sample calculation is provided in Appendix I.

Subjects

Six healthy male cyclists (height 1.77 ± 0.05 m, mass 71.9 ± 6.3 kg) volunteered for this investigation. All were experienced cyclists. Each subject was informed verbally and in writing of the requirements of the investigation, and each gave written informed consent.

Determination of Model Parameters

Aerodynamic Parameters. The aerodynamic drag force of each subject was measured in the Texas A&M wind tunnel in College Station, Texas. Drag force was measured using the tunnel's main mechanical balance. Force data were sampled at a rate of 100 Hz and averaged for 30 s for each measured value. Drag area was calculated from the drag force as described above ($C_D A = 2 F_D / \rho V_a^2$). Testing was conducted at an air velocity of approximately 13.4 m/s and at yaw angles (i.e., the angle of alignment between the bicycle and the air stream) of 0, 5, 10, and 15°. To accurately simulate riding conditions during wind tunnel testing, subjects pedaled at approximately 90 RPM, and the front wheel was rotated by a small electric motor.

Wind tunnel drag data were obtained for each subject while he sat upon the test bicycle. The bicycle was equipped with an adjustable handlebar stem and with aerodynamic handlebars with elbow supports. Each subject was positioned on the bicycle so that when he assumed the time trial position with elbows on the elbow rests, his shoulder joint was aligned approximately 5 cm above the hip joint (greater trochanter). The bicycle was equipped with a lens-shaped rear disk wheel and a front wheel with an airfoil-shaped cross-section and 24 oval spokes. The tires were 20 mm in cross-sectional width and inflated to a pressure of 9 atmospheres.

Measurement of Air Velocity and Direction. During each road-cycling trial (see Road Cycling Trials below), air velocity was measured by a cup anemometer (Young Mfg., Model 12102) located immediately adjacent to the course. The turning plane of the anemometer cups was located at approximately the same height as the subject's torso while positioned on the bicycle. Four to eight measurements of air velocity were made during each trial. Immediately following each road-cycling trial, the airport control tower was contacted by radio for information regarding wind direction.

Coefficient of Rolling Resistance. We did not measure rolling resistance directly. However, Kyle (1988) reported C_{RR} values ranging from 0.0027 to 0.0040 for 10 high-pressure clincher bicycle tires on smooth asphalt. Those tires were similar, but not identical, to those used on our test bicycle. Therefore, we used the average of those 10 values ($C_{RR} = 0.0032$) for our model.

Wheel Bearing Friction. The model parameters for wheel bearing friction were based on the values reported by Dahn et al. (1991) and incorporated into Equation 7.

Changes in Potential Energy. The parameters required for the potential energy terms were the bike and rider mass and the road gradient. The mass of the bike and rider was determined with a beam-balance scale. The road gradient for the section used in the road cycling trials was determined from construction plans and was found to be 0.3%.

Changes in Kinetic Energy. The kinetic energy at the beginning and end of each road cycling trial was determined based on the velocity recorded by the SRM at those time points.

Road Cycling Trials

Road cycling trials were conducted on a taxiway at the Easterwoods Airport, which is located adjacent to the wind tunnel facility in College Station, Texas. A fixed-distance test section was located between two easily seen landmarks. This section was measured three times with a distance wheel (Rolatape Corp., Model MM34) and found to be 471.8 m in length. The taxiway was straight and was aligned on a compass heading of 340 to 160°. The surface of the test section was concrete. There were no structures or other surface features within several hundred meters that might influence local wind velocity.

Ample distance was allowed beyond each end of the test section for subjects to accelerate and decelerate. Subjects were instructed to reach steady-state velocity before entering the test section for each trial. Once within the test section, the subjects were instructed to maintain constant velocity and were able to view their velocity on the SRM display. Each subject rode the test section in both directions at three different velocities (7, 9, and 11 m/s), and 1 subject rode at a fourth velocity (12 m/s), for a total of 38 trials. The subjects were timed from one end of the test section to the other to determine average velocity. Timing was performed with a hand-held stopwatch. The stopwatch was synchronized with the SRM timing so we could determine power during each road cycling trial test period.

Comparison of Modeled and Measured Power

For each road cycling trial, the model was used to calculate cycling power based on the measured air and ground velocity, road gradient, bike and rider mass, drag area, estimated rolling resistance, and frictional losses in the bearings and chain drive system. This calculated power was compared with the power recorded by the SRM power measurement system in two ways. First, linear regression was used to determine the relationship between measured and modeled power. Second, the absolute value of the difference be-

tween the values for modeled and measured power for each trial was used to determine the standard error of measurement.

Statistics

A paired Student's *t* test and linear regression were used to compare power delivered to the flywheel with power measured by the SRM. The effects of yaw angle on drag area were analyzed using ANOVA. A paired Student's *t* test and linear regression were used to compare power measured during the road cycling trials with power calculated by the mathematical model.

Results

Results from the SRM power measurement system are shown in Figure 1. Paired Student's *t* test indicated that the power measured by the SRM was significantly different ($p < .001$) than the power delivered to the Monark ergometer flywheel. Linear regression of power delivered to the flywheel versus SRM power showed that SRM power was related to flywheel power by the following equation: $\text{SRM power} = 1.023564 \times \text{flywheel power}$ ($R^2 > .99$). Interestingly, this 2.3564% difference is similar in magnitude to values for friction losses normally associated with chain drive systems. Therefore, for the modeling calculations below, it was assumed that the SRM power was valid and that the efficiency of the chain drive system (E_c) was 97.698%.

The results of wind tunnel testing of the subjects are shown in Table 1, expressed in drag area (m^2). Drag area tended to decrease slightly with increasing yaw angle, but ANOVA indicated that the differences were not significant.

The power measured by SRM and the power calculated by the mathematical model for all the road-cycling trials are shown in Figure 2. The power measured by the SRM and

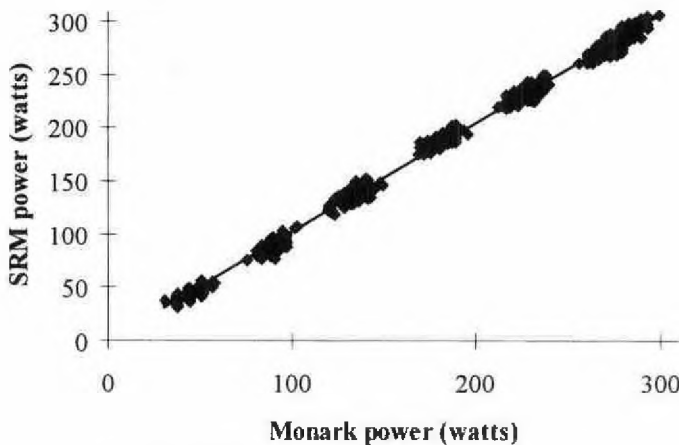


Figure 1 — SRM power meter validation. Power measured by the SRM was related to power delivered to the ergometer flywheel by the following equation: $\text{SRM power} = 1.023564 \times \text{flywheel power}$ ($R^2 = .997$), when the regression line was constrained to pass the origin. The inverse of the slope of the regression line (i.e., $1/1.023564 = 0.97698$) represents the efficiency of the chain drive system. Scatter in the data represents normal variation in power associated with minor changes in pedaling rate.

Table 1 Drag Area at Four Yaw Angles Calculated From Wind Tunnel Test Results

	Yaw angle (degrees)			
	0	5	10	15
Drag area (m ²)	0.269 ± 0.006	0.265 ± 0.008	0.265 ± 0.009	0.255 ± 0.008

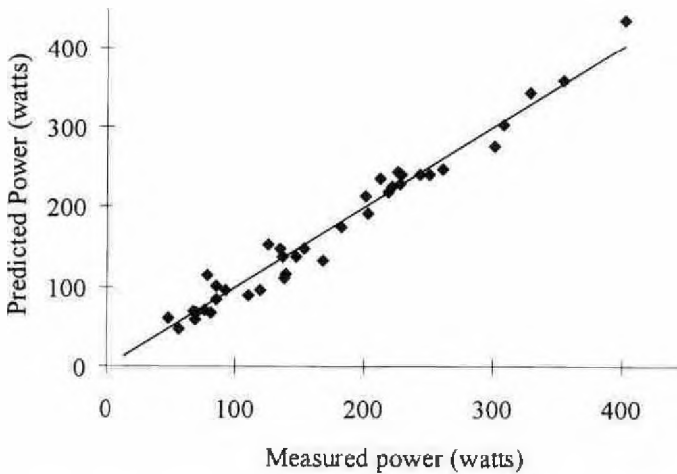


Figure 2 — Comparison of measured and modeled power. For all road cycling trials, the model power was related to the measured power by the following equation: Modeled power = 1.00 × measured power ($R^2 = .97$), when the regression line was constrained to pass through the origin.

the power predicted by the mathematical model were not different when compared using a paired Student's *t* test. Mean values were 172.8 ± 14.7 W for SRM versus 172.0 ± 15.2 W for the model. Linear regression indicated that the values for power measured by the SRM were highly correlated with the power calculated by the model (modeled power = $1.00 \times$ measured power, $R^2 = .97$). The standard error of measurement of the difference between the measured and modeled power was 2.7 W.

For each trial, the mean values of cycling velocity (V_c), air velocity (V_a), wind velocity (V_w), wind direction (D_w), power associated with aerodynamic drag (P_{AT}), rolling resistance (P_{RR}), bearing friction (P_{WB}), chain friction (P_c), and changes in kinetic (P_{KE}) and potential energy (P_{PE}) are shown in Table 2. Positive values for P_{PE} are associated with overcoming gravity when riding uphill, whereas negative values represent power put into the system by gravity when riding downhill.

Discussion

This investigation has demonstrated that road cycling power can be accurately measured and modeled. In our 38 road cycling trials, the standard error of measurement between modeled power and measured power was only 2.7 W. We believe that this validation is a necessary and primary step that must precede more complex modeling.

Table 2 Mean (\pm SD) Values for All 6 Subjects for Ground (V_G), Air (V_a), and Wind Velocity (V_w) and Wind Direction (D_w) for Each Component of Power During the Trials: Power Related to Potential Energy (P_{PE}), Wheel Bearings (P_{WB}), Rolling Resistance (P_{RR}), Aerodynamic Drag (P_{AT}), Kinetic Energy (P_{KE}), and Chain Friction (P_c), and for Modeled and Measured Power

	Bout 1		Bout 2		Bout 3		Bout 4		Bout 5		Bout 6	
	<i>M</i>	<i>SD</i>	<i>M</i>	<i>SD</i>	<i>M</i>	<i>SD</i>	<i>M</i>	<i>SD</i>	<i>M</i>	<i>SD</i>	<i>M</i>	<i>SD</i>
V_G (m/s)	6.8	0.3	7.0	0.3	8.8	0.3	9.1	0.3	10.9	0.4	11.1	0.6
V_a (m/s)	6.1	0.6	8.1	0.5	8.2	0.7	9.6	0.4	10.4	0.7	12.1	0.5
V_w (m/s)	2.3	0.3	2.6	0.3	2.4	0.3	2.2	0.4	2.4	0.4	2.6	0.2
D_w (compass heading in degrees)	222	16	222	16	227	19	225	16	227	19	222	16
P_{PE} (W)	16.5	0.7	-16.9	0.8	21.2	0.7	-22	0.9	26.3	0.8	-26.7	1.2
P_{WB} (W)	1.0	0.0	1.1	0.0	1.5	0.0	1.6	0.0	2.0	0.0	2.1	0.1
P_{RR} (W)	18.2	0.8	18.6	0.9	23.3	0.7	24.2	1	29	0.8	29.4	1.3
P_{AT} (W)	45.5	7.6	75.6	10	98.6	15.7	137	14.3	193	22.9	269	33.5
P_{KE} (W)	-2.2	1.2	1.4	0.7	-0.6	1	0.9	0.6	-1.4	3.1	-0.6	4.2
P_c (W)	1.9	0.2	2	0.2	3.5	0.4	3.5	0.3	6.1	0.5	6.7	0.8
Modeled power (W)	81	8	82	10	147	17	145	14	255	22	280	33
Measured power (W)	81	13	77	5	151	16	156	13	251	22	273	30

Our model was based on fundamental engineering and physical principles and was similar in many ways to models proposed by previous investigators (Davies, 1980; Di Prampero et al., 1979; Kyle, 1988; Olds et al., 1995, 1993). The main difference in this investigation was that we were able to accurately measure the cycling power and the drag area of our subjects and either directly measure or reliably estimate all other model parameters. This combination of factors allowed us to calculate, with great detail and accuracy, the forces acting on our subjects during the road cycling trials.

A previous model by Olds et al. (1995) accounted for 79% of the variation in time trial performance. That seems quite impressive, especially considering that one of the most important parameters, bike and rider drag area, was estimated from anthropometric dimensions. The present model accounted for over 97% of the variation in cycling power. Although we did not attempt to model the human power input, that is a logical topic for further investigation. For instance, Coyle et al. (1991) showed that power during a 1 hr cycle ergometer performance trial and power at lactate threshold were highly associated with road time trial performance. Consequently, we would expect that those measures might be strong predictors of road cycling power, and hence, using our model, time trial performance.

Validation of our mathematical model was contingent upon power measurement during road cycling. Power measured by the SRM system was significantly different than the power delivered to the ergometer flywheel. However, the difference (2.36%) was characteristic of power loss in chain drive systems (Kyle, 1988; Whitt & Wilson, 1982). Thus,

it seems reasonable to assume that the SRM provides a valid measure of power that differs from the power delivered to the ergometer flywheel only by an amount lost to chain friction. Consequently, we have assumed that the SRM is in fact valid and accurate and that the difference is related to chain efficiency.

Most of the power produced by the subjects was used to overcome aerodynamic losses, which accounted for losses equivalent to 56–76% and 93–96% of the total power for trials in the uphill and downhill directions, respectively. The proportion of power to overcome aerodynamic drag relative to total power increased with increased speed. The course for our trials was very nearly flat (0.3% grade), but changes in potential energy accounted for 10–20% of total power. During trials in the uphill direction, changes in potential energy accounted for losses equivalent to 10–20% of the total power. For trials in the downhill direction, changes in potential energy added an equivalent amount of power to the system that could then be used to overcome losses due to other power sources (note that this is the reason for the large discrepancy between the percentage of aerodynamic losses in the uphill and downhill directions). The 10–20% magnitude of power loss related to changes in potential energy seems remarkable, considering the very small road grade, and suggests that potential energy changes may account for much higher portions of power on more varied terrain. The results (Table 2) indicate that the power during uphill and downhill trials was quite similar for each speed. However, this was coincidental and occurred because the downhill direction tended to be into the wind whereas the uphill direction tended to be with the wind. Rolling resistance accounted for 10 to 20% of total power, and the proportion of rolling resistance power to total decreased with increased speed. The changes in kinetic energy were approximately 1% of total power (1 to 2 W) and demonstrated that our subjects were able to maintain very nearly stable velocity across the test section. Bearing friction losses were also approximately 1% of total power (1 to 2 W). Losses due to drive chain efficiency were fixed at 2.36% for all trials and accounted for 2 to 7 W.

Wind velocity was measured at one site on the course and at several discrete intervals during each bout. Those discrete measures showed a high degree of variability within each bout, with the standard deviation of wind velocity within each bout averaging 0.4 m/s. Also, wind direction was only obtained at the end of each bout and was measured at the airport control tower, located approximately 800 m away from the test section. Air density was measured at the wind tunnel, some 800 m away from the location of the road cycling trials. It was only measured prior to the road cycling trials and was assumed to remain constant throughout the test period. Even though the differences in our measured and modeled power were small, it seems that these limitations in the measurement of air density, wind direction, and wind velocity may have produced much of that variability.

Each trial was performed under highly controlled conditions: near-steady-state velocity, one direction, and constant grade. A more robust method to consider for future research might include more varied terrain in a "real-world" riding situation, which would include hills and changes in direction.

Model Application

Having established the validity of our model, we were interested in using it to predict the effects of different values for wind velocity, road gradient, rolling resistance, and drag area. For all of the following modeling, we used a hypothetical subject who had the average characteristics of our subjects (drag area = 0.264 m², mass = 71.9 kg). The power required for such a hypothetical subject to ride at 11 m/s on a flat surface in calm wind

conditions was found to be 255 W, and that power was used in all of the following examples.

Wind Velocity. The effects of wind velocities of 0–10 m/s directly with and against the direction of travel are shown in Figure 3. Even though the equations governing these calculations are quite complex, the results show that wind velocity affects cycling velocity in a very nearly linear manner (cycling velocity = $11.33 - 0.62 \times V_{\text{WTAN}}$, $R^2 > .99$). Thus, it appears that when a rider is cycling at 255 W, the wind affects riding velocity by approximately 62% of the tangential wind velocity.

Road Gradient. During our road cycling trials, the power related to changes in potential energy (P_{PE}) accounted for 10–20% of total power. The grade for the test course was only 0.3%, and we did not anticipate that the small grade would have such an impact on cycling power. We wondered about the effects of increased grade on cycling power, and so we used our model to determine the effects of climbing and descending grades of up to 6%. The results of this modeling, shown in Figure 4, indicate that for cycling at 255 W, each 1% of grade increases or decreases cycling velocity by about 1.24 m/s (approximately 11%). As with the effects of wind described above, the effects of road grade are very nearly linear (cycling velocity = $11.26 - 1.25 \times \text{road gradient}$, $R^2 > .99$) over the range of road gradients modeled.

Rolling Resistance. During our road cycling trials, the power dissipated to rolling resistance accounted for 10–20% of total power. We estimated that our tires had a coefficient of rolling resistance (C_{RR}) of .0032 based on reported values for similar tires. Reported values for C_{RR} for other tires vary widely, from .0016 for a silk track-racing tire to .0066 for a touring tire (Whitt & Wilson, 1982). Therefore, we used our model to evaluate the effects of C_{RR} across that range. The results of this modeling, shown in Figure 5, indicate that cycling velocity varies nearly linearly with C_{RR} (cycling velocity = $11.46 - 142 \times C_{\text{RR}}$, $R^2 > .99$). Over the range of C_{RR} evaluated, rolling resistance could affect cycling velocity by up to 6%.

Effects on Cycling Performance. On first inspection it might seem that the effects of wind and road gradient would “average out” during the course of a loop or out-and-back

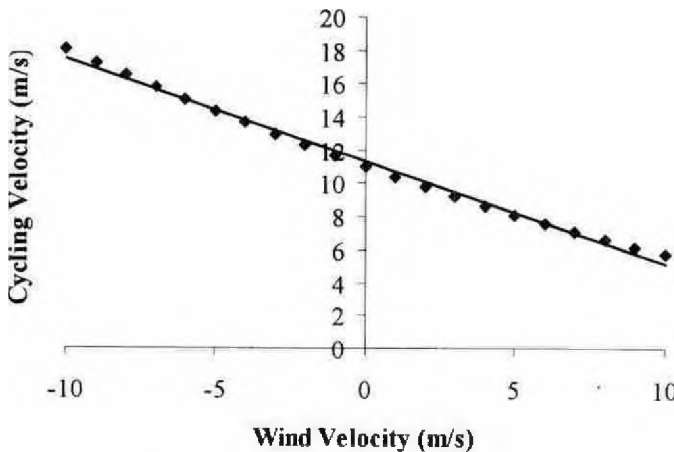


Figure 3 — The effects of wind velocity on cycling velocity at 255 W. Within the range of wind velocities evaluated (–10 to 10 m/s), the effects on cycling velocity were very nearly linear (cycling velocity [m/s] = $11.33 - 0.62 \text{ wind velocity [m/s]}$, $R^2 > .99$).

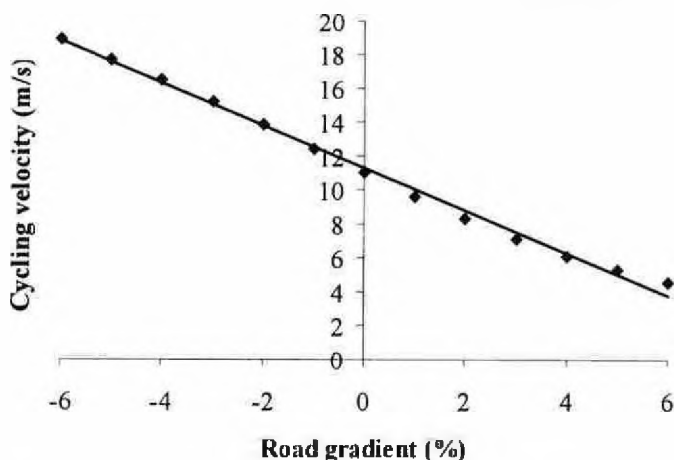


Figure 4 — The effects of road gradient on cycling velocity. Within the range of road gradients evaluated (-6 to 6%), the effects on cycling velocity were very nearly linear (cycling velocity [m/s] = 11.26 - 1.25 road gradient [%], $R^2 > .99$).

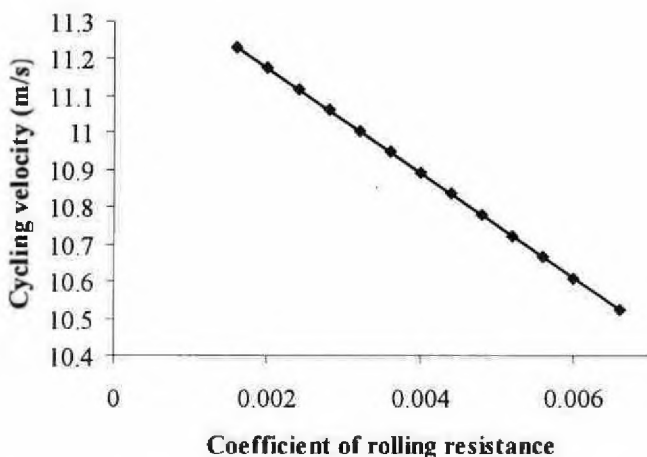


Figure 5 — The effects of rolling resistance on cycling velocity. Within the range of coefficient of rolling resistance values evaluated (0.0016 to 0.0066), the effects on cycling velocity were very nearly linear (cycling velocity [m/s] = 11.46 - 142 C_{RR} [dimensionless], $R^2 > .99$).

course. Although it is true that those effects will increase or decrease cycling velocity by about the same amount, the same is not true for performance time. Consider the effects of a 4 m/s wind on a 40 km time trial with an out-and-back course. In calm conditions, the velocity would be 11 m/s in both directions and the total performance time would be 60:36. However, if the rider encountered a 4 m/s headwind in one direction, velocity would be reduced to 8.63 m/s and the rider would require 38:37 to cover 20 km. On the return portion of the course the rider would benefit from the tailwind, velocity would increase to 13.67 m/s, and the rider would require only 24:24 to cover 20 km. Even though the magnitude of the

two velocities would average 11.15 m/s, the average speed for the out-and-back course would be only 10.58 m/s and performance time would be increased by about 5% to 63:01. Similarly, an out-and-back course with a 2% grade would increase 40 km time approximately 7% from 60:36 to 64:36.

Drag Area. Much attention has been focused on cycling performance improvement due to reductions in aerodynamic drag. The bicycle used in this investigation was of high quality and the body positions adopted by our subjects allowed their torsos to be quite nearly horizontal. However, neither the bicycle nor the body positions were as extreme as some of those used in the 1996 Olympics. Those games became somewhat of a showcase for the latest and sleekest designs. We wondered how changes in drag area of up to 20% would affect cycling velocity. Therefore, we used our model to determine the effects of cycling at 255 W on a flat surface, in calm winds with drag areas of 0.211 to 0.317 m². The results of this modeling, shown in Figure 6, indicate that these changes in drag area would increase or decrease cycling velocity by up to 0.71 m/s or about 6.4%.

The mathematical model for cycling power requires a complex, third-order, polynomial equation with several parameters. Even so, when cycling power was held constant, wind velocity, road grade, rolling resistance, and drag area each affected cycling velocity in a quite nearly linear manner ($R^2 > .99$) over the range of values evaluated. This finding allows for a simplified understanding of the effects of those parameters. For instance, the findings that wind affects cycling velocity by about two-thirds of the wind velocity, and that road gradient affects cycling velocity by about 11% for every 1% change in road gradient, will allow athletes and coaches to have a simplified but realistic expectation of how environmental conditions should affect performance. Similarly, the finding that every 0.01 m² reduction in drag area increases cycling velocity by about 0.13 m/s may motivate athletes and sport scientists to work toward lowering aerodynamic drag.

The purpose of this investigation was to determine if cycling power, measured during actual road cycling, can be accurately predicted by a mathematical model. It was established that the SRM power-meter system provided power measurements that differed from the power delivered to an ergometer flywheel by an amount typical of losses in

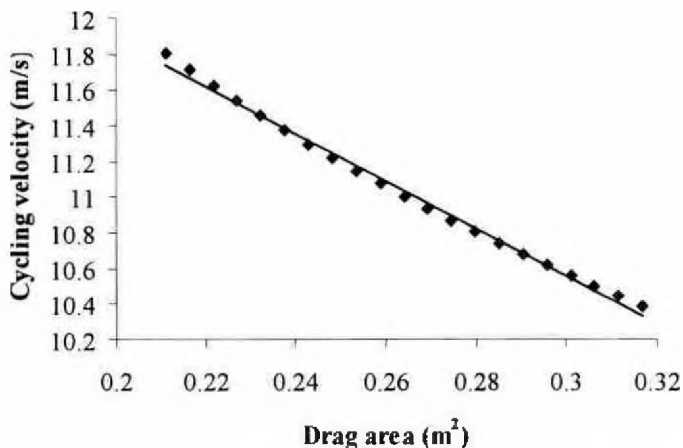


Figure 6 — The effects of drag area on cycling velocity. Within the range of drag area values evaluated (0.211 to 0.317 m²), the effects on cycling velocity were very nearly linear (cycling velocity [m/s] = 14.5 - 13.3 C_dA [m²], $R^2 > .99$).

chain drive systems. We interpreted this finding to mean that the SRM power measurement system provided a valid measure of cycling power. A mathematical model of cycling power based on engineering and physical principles was derived, and values for each parameter in the model were determined. Comparison of the power values predicted by the model with the values that were measured directly confirmed that the model was a valid and accurate representation of cycling power. Applications of the model to various practical questions regarding model parameters indicated that each parameter affected cycling velocity in a very nearly linear manner. Therefore, this investigation effectively addressed the most basic question regarding the modeling of cycling performance, and it can now be stated that a mathematical model can, in fact, accurately predict power and velocity during road cycling.

References

- Coyle, E.F., Feltner, M.E., Kautz, S.A., Hamilton, M.T., Montain, S.J., Baylor, A.M., Abraham, L.D., & Petrek, G.W. (1991). Physiological and biomechanical factors associated with elite endurance cycling performance. *Medicine & Science in Sports & Exercise*, **23**(1), 93-107.
- Dahn, K., Mai, L., Poland, J., & Jenkins, C. (1991). Frictional resistance in bicycle wheel bearings. *Cycling Science*, **3**(3), 28-32.
- Davies, C.T. (1980). Effect of air resistance on the metabolic cost and performance of cycling. *European Journal of Applied Physiology & Occupational Physiology*, **45**(2-3), 245-254.
- Di Prampero, P.E., Cortili, G., Mognoni, P., & Saibene, F. (1979). Equation of motion of a cyclist. *Journal of Applied Physiology*, **47**(1), 201-206.
- Fox, R.W., & McDonald, A.T. (1973). *Introduction to fluid mechanics* (2nd ed.). New York: Wiley.
- Hooker, D., & Spangler, G. (1989). Scientific performance testing. *Cycling Science*, **1**(1), 2-5.
- Kyle, C.R. (1988). The mechanics and aerodynamics of cycling. In E.R. Burke (Ed.), *Medical and scientific aspects of cycling* (pp. 235-251). Champaign, IL: Human Kinetics.
- Olds, T.S., Norton, K.I., Lowe, E.L., Olive, S., Reay, F., & Ly, S. (1995). Modeling road-cycling performance. *Journal of Applied Physiology*, **78**(4), 1596-1611.
- Olds, T.S., Norton, K.I., & Craig, N.P. (1993). Mathematical model of cycling performance. *Journal of Applied Physiology*, **75**(2), 730-737.
- Rysehon, T.W. (1994). Physiologic aspects of bicycling. *Clinics in Sports Medicine*, **13**(1), 15-38.
- Schoberer, E. (1994). *Operating instructions for the SRM training system*. Welldorf, Germany.
- Wheeler, J.B., Gregor, R.J., & Broker, J.P. (1992). A dual piezoelectric bicycle pedal with multiple shoe/pedal interface compatibility. *International Journal of Sport Biomechanics*, **8**, 251-258.
- Whitt, F.R., & Wilson, D.G. (1982). *Bicycling science*. Cambridge, MA: MIT Press.

Appendix I: Sample Calculation of Power

The raw data recorded for each test are shown below. These data, in conjunction with the model parameters (i.e., coefficient of rolling resistance, drag area, bearing friction, and drive chain efficiency), were used to calculate the estimated power for each trial as shown below.

Rider mass	80 kg
Bicycle mass	10 kg
Wind direction	310°
Wind velocity	2.94 m/s
Time to cover 471.8 m	56.42 s
Initial velocity	8.28 m/s
Final velocity	8.45 m/s
Ride direction	340
Grade	0.003

Calculated values:

$$\begin{aligned} \text{Ground velocity } V_G &= 471.8 \text{ m}/56.42 \text{ s} = 8.36 \text{ m/s} \\ \text{Air velocity } V_{WIND} &= 2.94 \text{ m/s} \text{ COS}(340 - 310) = 2.55 \text{ m/s} \\ V_a &= V_G + V_{WIND} = 8.36 + 2.55 = 10.91 \text{ m/s} \\ \text{Yaw angle } V_{WNOR} &= 2.94 \text{ m/s} \text{ SIN}(340 - 310) = 1.47 \text{ m/s} \\ \text{Yaw} &= \text{TAN}^{-1}(1.47/10.91) = 7.7^\circ \end{aligned}$$

Drag area based on yaw angle: For this subject, drag area at 5 and 10° was 0.258 and 0.257, respectively. Interpolation to a yaw angle of 7.7° yields the corrected drag area:

$$C_D A = [(0.257 - 0.258)/(10 - 5)] (7.7 - 5) + 0.257 = 0.2565$$

$$\text{Aerodynamic power: } P_{AD} = V_a^3 V_G / 2 \rho (C_D A + F_w) = 10.91^2 \times 8.36 \times 0.5 \times 1.2234 \times (0.2565 + 0.0044) = 158.8 \text{ W}$$

$$\text{Rolling resistance power: } P_{RR} = V_G \text{ COS}[\text{TAN}^{-1}(G_R)] C_{RR} m_t g = 8.36 \times \text{COS}[\text{TAN}^{-1}(0.003)] \times 0.0032 \times 90 \times 9.81 = 23.6 \text{ W}$$

$$\text{Wheel bearing friction power: } P_{WB} = V_G (91 + 8.7 V_G) 10^{-3} = 8.36 \times (91 + 8.7 \times 8.36) 10^{-3} = 1.4 \text{ W}$$

$$\text{Power related to changes in potential energy: } P_{PE} = V_G m_t g \text{ SIN}[\text{TAN}^{-1}(G_R)] = 8.36 \times 90 \times 9.81 \times \text{SIN}[\text{TAN}^{-1}(0.003)] = 22.1 \text{ W}$$

$$\text{Power related to changes in kinetic energy: } P_{KE} = 1/2 (m_T + I/r^2) \times (V_{off}^2 - V_G^2) / (t_1 - t_2) = 1/2 \times (90 + 0.14/0.311^2) \times (8.45^2 - 8.28^2) / 56.42 = 2.3 \text{ W}$$

$$\text{Net power: } P_{NET} = 158.8 + 23.6 + 1.4 + 22.1 + 2.3 = 208.2 \text{ W}$$

$$\text{Total power: } P_{TOT} = P_{NET} / E_C = 208.2 / 0.976 = 213.3 \text{ W}$$

For this bout the SRM power averaged 218 W.

Acknowledgments

We would like to thank the subjects for their enthusiastic participation. We are very grateful to the members of the Easterwoods Airport staff for their invaluable help and cooperation. Also, we thank Mr. Sandy Liman of Allsop/Soltride for funding the wind tunnel testing, and Mr. Nick Chenoweth of Electronic Data Systems, who provided the bicycle and SRM used in this investigation and partial funding.